

SUPPLEMENTARY MATERIAL

Oleonolic Acid as Active Antidiabetic Component of *Xylopia aethiopica* (Annonaceae) Fruit: Bioassay guided isolation and molecular docking studies

Aminu Mohammed^{1,3}, Gbonjubola Victoria Awolola², Mohammed Auwal Ibrahim³, Neil Anthony Koorbanally² and Md. Shahidul Islam^{1*}

¹Department of Biochemistry, School of Life Sciences and ²Department of Chemistry, School of Chemistry and Physics, University of KwaZulu-Natal, (Westville Campus), Durban, 4000, South Africa

³Department of Biochemistry, Faculty of Life Sciences, Ahmadu Bello University, Zaria-Nigeria

***Corresponding author:**

Prof. Md. Shahidul Islam

School of Life Sciences

University of KwaZulu-Natal (Westville Campus)

Durban 4000, South Africa.

Tel: +27 31 260 8717, Fax: +27 31 260 7942

Email: islamd@ukzn.ac.za or sislam1974@yahoo.com

Abstract

The present study was designed to conduct the bioassay-guided isolation of possible bioactive compound(s) responsible for the antidiabetic action of *Xylopia aethiopica* (Dunal) A. Rich. fruit. The isolation of compound was guided by α -glycosidase and α -amylase inhibitory activities. Molecular docking with Autodock Vina was used to decipher the mode of interaction and binding affinity of the possible compound(s) with the selected enzymes. A pentacyclic triterpene, oleanolic acid (OA) was isolated from *X. aethiopica* fruit and exhibited significantly ($P < 0.05$) lower IC_{50} values (α -amylase: $89.02 \pm 1.12 \mu M$, α -glucosidase: $46.05 \pm 0.25 \mu M$). Interestingly, OA was found to bind to the α -amylase and α -glucosidase with minimum binding energy of -0.9

and -1.2 kcal/mol respectively and none of the interactions involved hydrogen bond formation. It was concluded that OA is responsible for the antidiabetic action of *X. aethiopica* fruit through the inhibition of α -amylase and α -glucosidase activities.

Keywords: Oleanolic acid, α -amylase, α -glucosidase, molecular docking

Oleanolic acid (OA)

Figure S1. ^1H NMR spectrum of oleanolic acid (OA) (CDCl_3 , 400 MHz).

Figure S2. ^{13}C NMR spectrum of oleanolic acid (OA) (CDCl_3 , 400 MHz).

Figure S3. DEPT spectrum of oleanolic acid (OA).

Figure S4. HMBC NMR spectrum of oleanolic acid (OA).

Figure S5. HSQC NMR spectrum of oleanolic acid (OA)

Figure S6. NOESY NMR spectrum oleanolic acid (OA).

Figure S7: Structure of oleanolic acid (OA) isolated from *X. aethiopica* fruit

Figure S8. Lineweaver-Burke plot for α -amylase (A) and α -glucosidase (B) in the absence and presence of the inhibitors (oleanolic acid).

Figure S9: Mode of interaction of oleanolic acid with human α -amylase (A) and human α -glucosidase (B). The red box areas signify the active site of the enzyme whilst the white boxes indicate the respective binding sites of the oleanolic acid showing the unusual conformation of the compound

Table S1. Kinetic analysis of α -amylase and α -glucosidase inhibition by oleanolic acid isolated from *X. aethiopica* fruit.

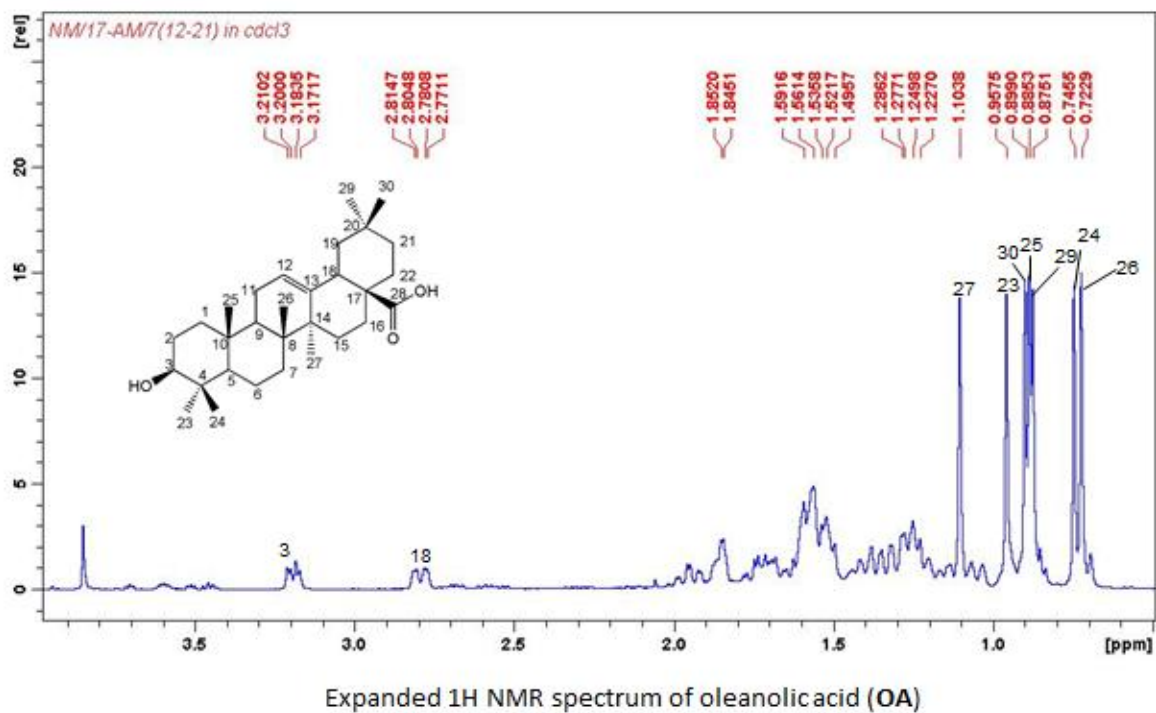


Figure S1. ^1H NMR spectrum of oleanolic acid (OA) (CDCl_3 , 400 MHz).

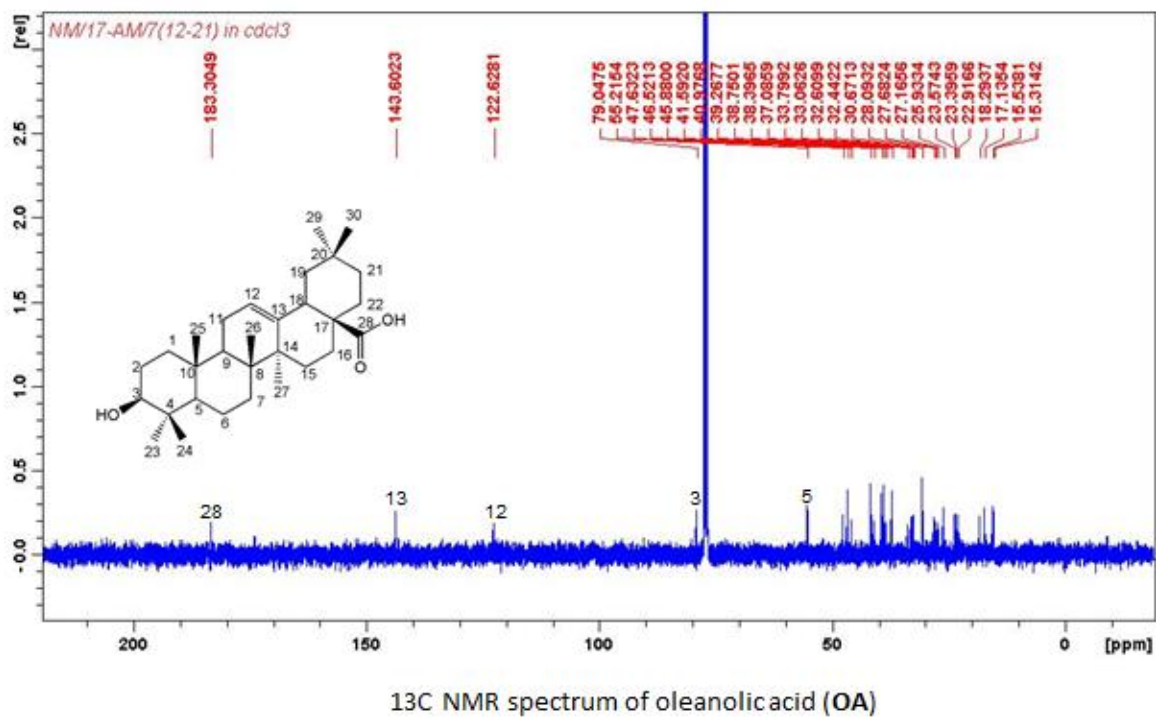


Figure S2. ^{13}C NMR spectrum of oleanolic acid (OA) (CDCl_3 , 400 MHz).

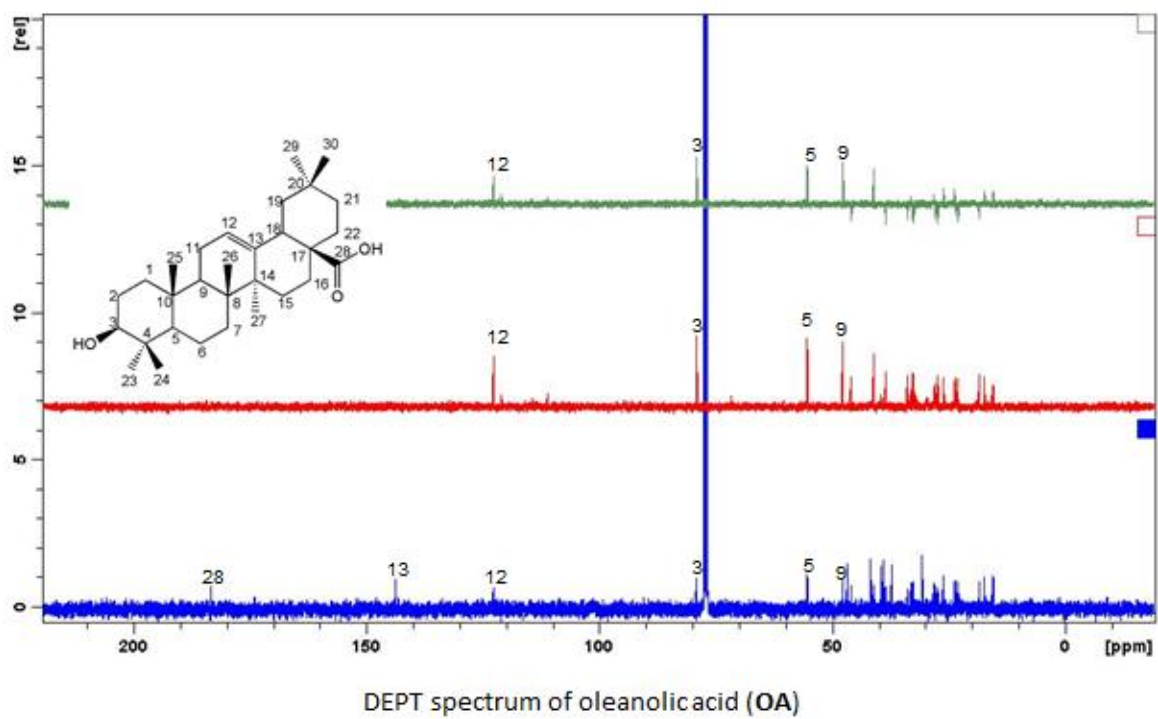


Figure S3. DEPT spectrum of oleanolic acid (OA).

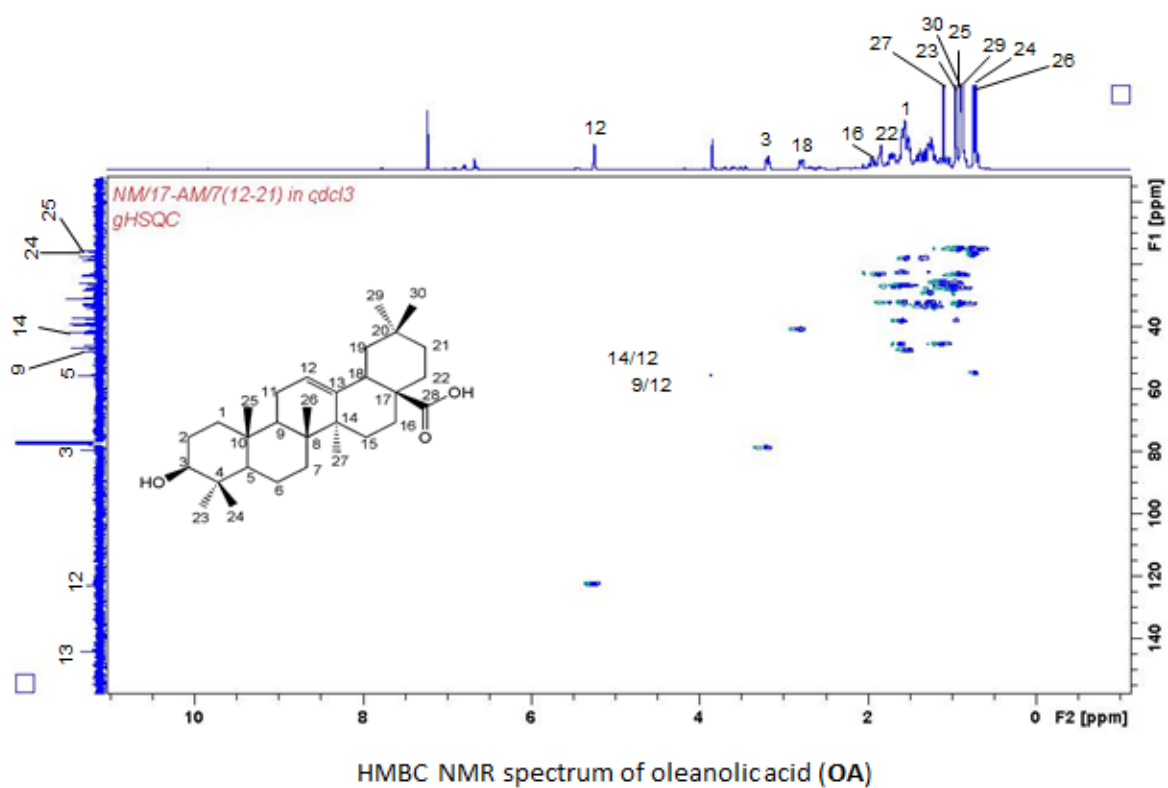


Figure S4. HMBC NMR spectrum of oleanolic acid (OA).

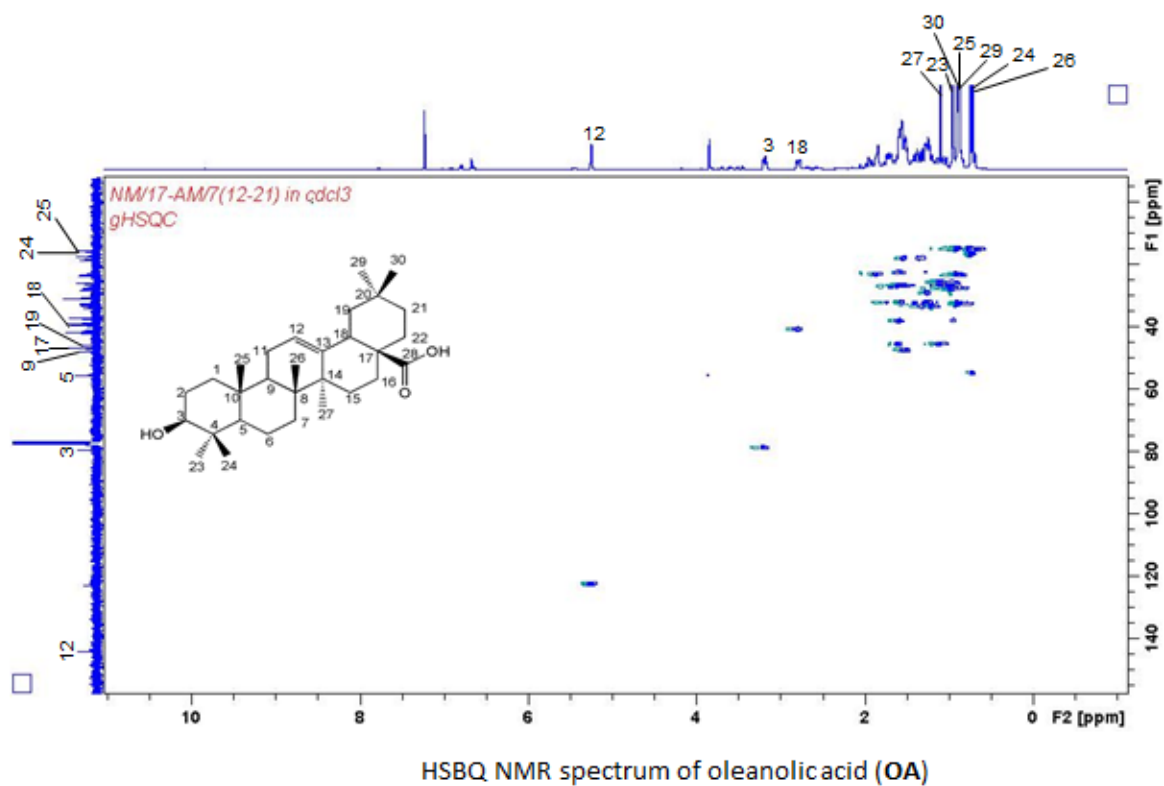


Figure S5. HSQC NMR spectrum of oleanolic acid (OA)

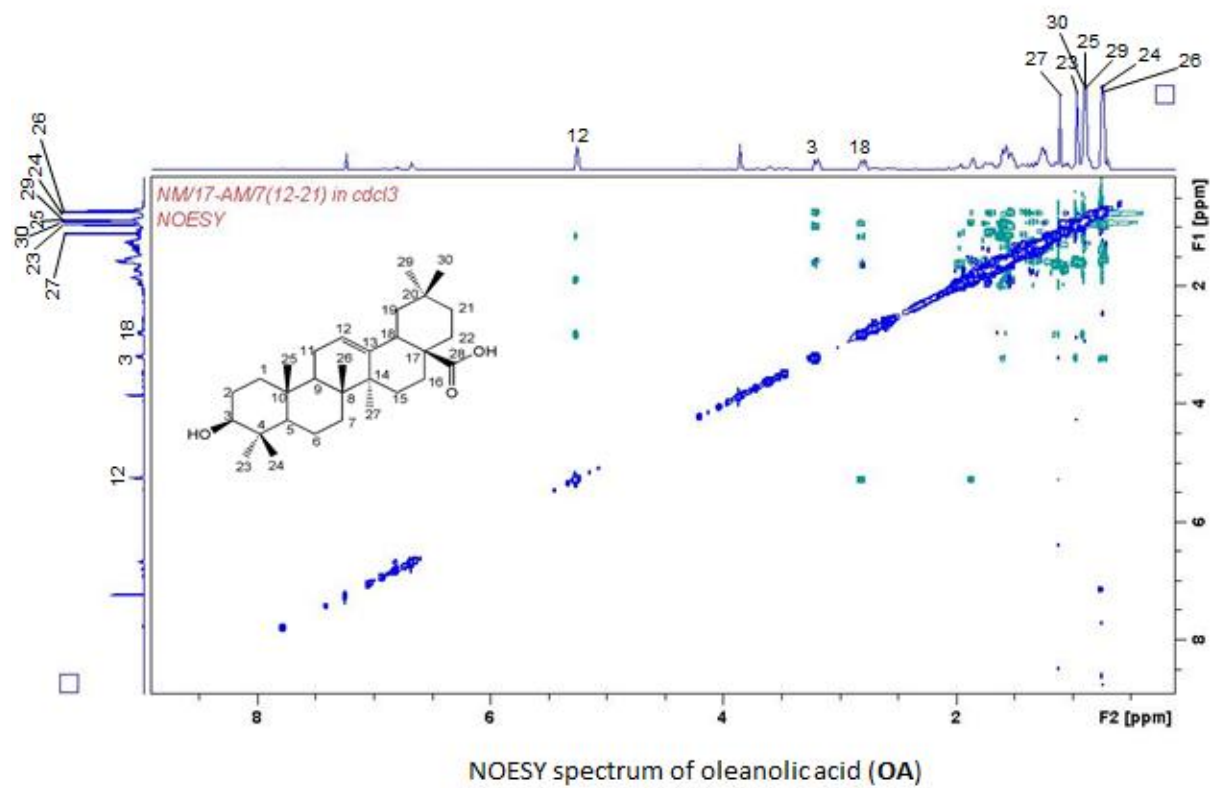


Figure S6. NOESY NMR spectrum oleanolic acid (OA).

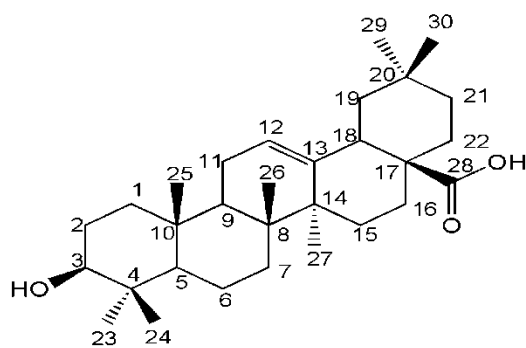


Figure S7: Structure of oleanolic acid (OA) isolated from *X. aethiopica* fruit

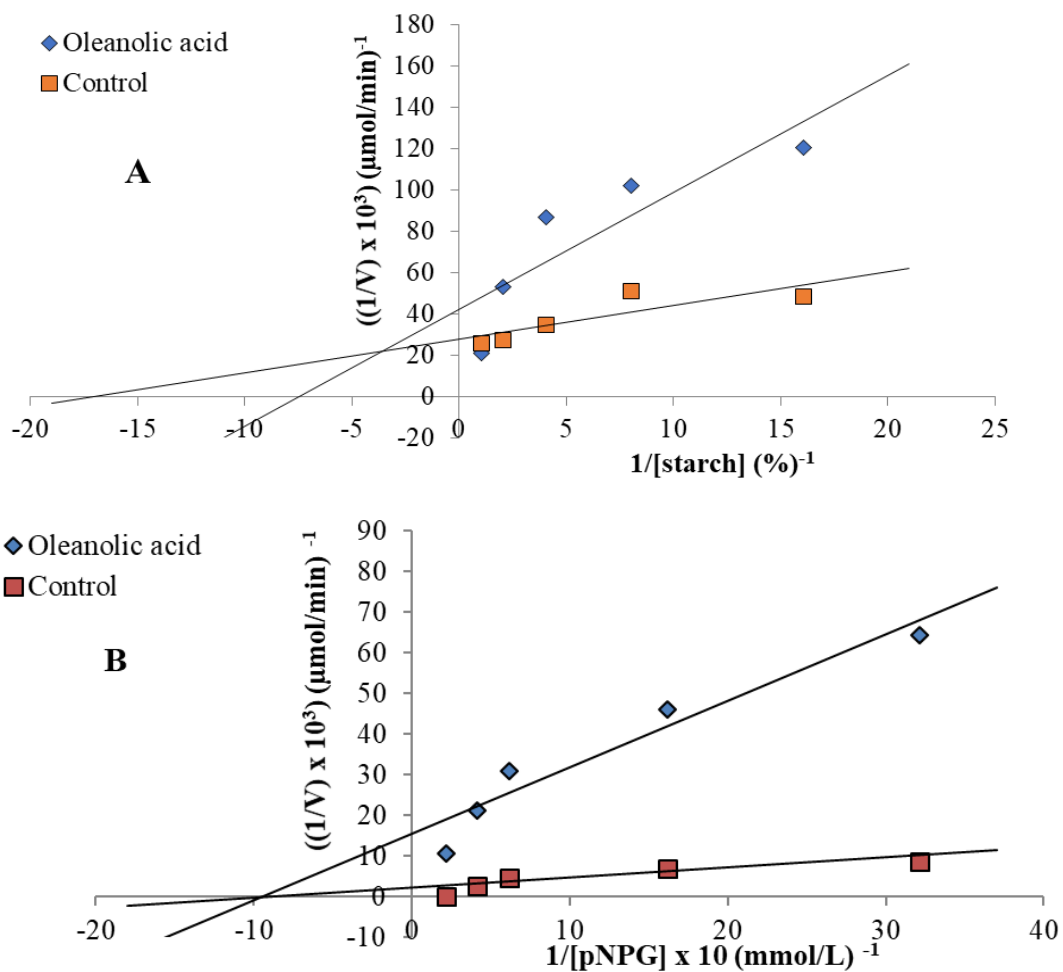


Figure S8. Lineweaver-Burke plot for α -amylase (A) and α -glucosidase (B) in the absence and presence of the inhibitors (oleanolic acid).

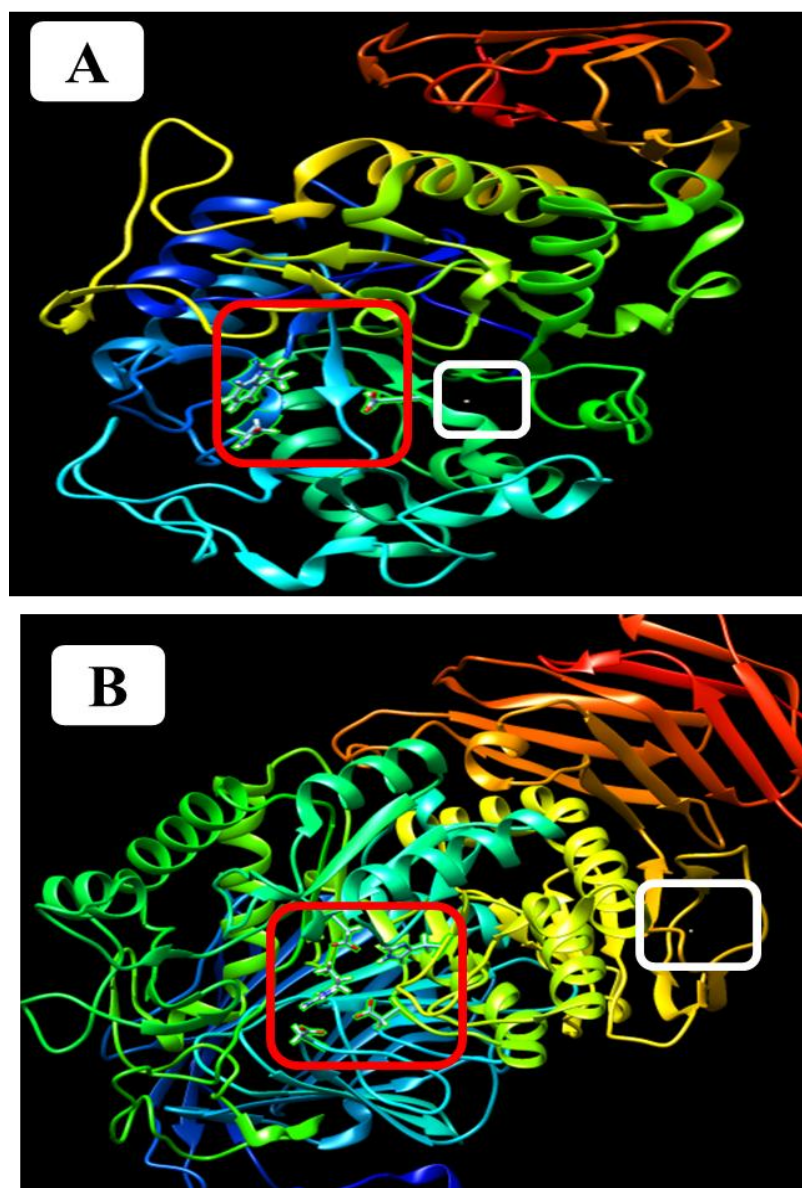


Figure S9: Mode of interaction of oleanolic acid with human α -amylase (**A**) and human α -glucosidase (**B**). The red box areas signify the active site of the enzyme whilst the white boxes indicate the respective binding sites of the oleanolic acid showing the unusual conformation of the compound

Table S1: Kinetic analysis of α -amylase and α -glucosidase inhibition by oleanolic acid isolated from *X. aethiopica* fruit.

Compounds	α -Amylase inhibition			α -Glucosidase inhibition		
	K_M (%)	V_{max} ($\mu\text{mol/min}$)	K_i ($\mu\text{g/mL}$)	K_M (mM)	V_{max} ($\mu\text{mol/min}$)	K_i ($\mu\text{g/mL}$)
Control	0.04	35.65		1.11	472.25	
Oleanolic acid	0.04	272.05	62.05	1.11	66.50	3.96

Materials and methods

Materials

Saccharomyces cerevisiae α -glucosidase (E.C. 3.2.1.20), porcine pancreatic α -amylase (E.C. 3.2.1.1), *p*-nitrophenyl glucopyranoside (*p*NPG), and *p*-nitrophenol were obtained from Sigma-Aldrich through Capital Lab Supplies, New Germany, South Africa. Starch, dinitrosalicylic acid (DNS), maltose, absolute ethanol, and ethyl acetate were obtained from Merck Chemical Company, Durban, South Africa.

Plant material

The fruit of *X. aethiopica* was freshly collected in December, 2012 from Ibadan, Oyo State, Nigeria and authenticated at the herbarium unit of the Biological Science Department, Ahmadu Bello University, Zaria, Nigeria by Mr. Umar Gallah. A voucher specimen number 1026 was deposited accordingly. The sample was immediately washed and shade-dried for 2 weeks to constant weight. The dried sample was ground to a fine powder and stored in airtight containers for transport to the University of KwaZulu-Natal, Westville Campus, Durban, South Africa for further investigations.

Preparation of plant extracts

Extraction of the sample was carried out according to the previously reported method (Ibrahim and Islam, 2014). In brief, the fine powdered *X. aethiopica* fruit (3 kg) was defatted with 10 L *n*-hexane. The defatted sample was extracted sequentially with ethyl acetate, ethanol and water by soaking for 48 h and filtered through Whatmann filter paper (No.1). The extracts obtained was then evaporated under vacuum, using a rotary evaporator (Buchi Rotavapor II,

Buchi, Germany) at 40 °C under reduced pressure to obtain the crude ethyl acetate, ethanol and water extracts which yielded 2.05%, 7.05% and 3.15%, respectively. The ethanol extract showed greater inhibition on the activities of α -glucosidase (IC_{50} : 162.25 \pm 7.06 μ g/mL) and α -amylase (IC_{50} : 210.02 \pm 10.30 μ g/mL) and hence, selected for the subsequent analysis, when the other extracts showed IC_{50} >500 μ g/mL for all the assays. Forty grams (40 g) of the crude ethanol extract of the fruit was dissolved in 500 ml of distilled water:methanol (9:1) and successively partitioned with *n*-hexane(2 x 500 ml), dichloromethane (2 x 500 ml), ethyl acetate (2 x 500 ml) and acetone (2 x 500 ml). The fractions were evaporated to dryness under vacuum at 40 °C whereas the remaining aqueous fraction was dried in a water bath at 50 °C. The dried fractions were transferred to microtubes and stored at 4 °C until further analysis. The *X. aethiopica* acetone sub-extract was a dark brownish residue and demonstrated the highest *in vitro* α -glucosidase (IC_{50} : 86.23 \pm 0.30 μ g/mL) and α -amylase (IC_{50} : 155.41 \pm 1.83 μ g/mL) inhibitory activities amongst the other sub-extracts and thus, it was selected for the isolation of possible bioactive compounds.

Isolation of bioactive compounds from the acetone sub-extract

A portion of the acetone sub-extract of *X. aethiopica* fruit (16 g) was fractionated on a 3.5 cm diameter column over silica gel (0.040-0.063 mm) using a gradient elution of *n*-hexane: EtOAc (with 10% increments of EtOAc) and then MeOH (100%) resulting in sixty-four (64) fractions. The column fractions were pooled together on the basis of TLC profiles to afford six (6) major fractions (A: 6-8; B: 9-13; C: 14-16; D: 18-22; E: 27-32 and F: 33-54). Fraction C (440.7 mg) demonstrated significantly ($P < 0.05$) the least IC_{50} values for α -amylase and α -

glucosidase inhibitory actions and was further purified with n-hexane: EtOAc (7:3). This yielded compound 1 (1.55 g).

All NMR (^1H , ^{13}C and 2D) experiments were recorded on a Bruker Avance III 400 MHz spectrometer. Sample was acquired with deuterated chloroform (CDCl_3). The spectra were referenced according to the deuteriochloroform signal at δH 7.24 (for ^1H NMR spectra) and δC 77.0 (for ^{13}C NMR spectra) for CDCl_3 .

Inhibition and kinetic studies of α -amylase (E.C. 3.2.1.1) and α -glucosidase (E.C. 3.2.1.20) actions

The α -amylase inhibitory effect of the compound was determined using a method of McCue and Shetty (2004) whereas the α -glucosidase activity was determined according to the method described by Kim et al (2005) using α -glucosidase from *S. cerevisiae*. For the, kinetic study, the same protocols were used except that the concentration of the compound was fixed at 30 $\mu\text{g/mL}$ with a variable concentration of substrates. The initial velocity data obtained were used to construct Lineweaver-Burke's plot to determine the K_M (Michaelis constant) and V_{max} (maximum velocity) of the enzyme as well as the K_i (inhibition binding constant as a measure of affinity of the inhibitor to the enzyme) and the type of inhibition for both enzymes.

Molecular docking studies

The crystal structure of α -amylase and α -glucosidase were retrieved from Protein Data Bank with PDB ID 4GQR and 34LY respectively, co-crystalised with myricetin and NR4-8II which are located in active sites of the respective enzymes. The protein structures were prepared as receptors by removing the co-crystallised ligands and water molecules for the preparation of

the docking by adding and polar hydrogen and Gasteiger charges using Chimera software (www.cgl.ucsf.edu/chimera/). The ligand was also subjected to the same dock prep tool in the Chimera. The structures of the receptors and the ligand were retrieved as pdb formats after the dock prep. Thereafter, the PDB prepared versions was subjected to Autodock Vina (Trott and Olson, 2010) using a final size space dimension, $x=41\text{\AA}$, $y=45\text{\AA}$ & $z=347\text{\AA}$, and centre 9.4, 30.41 and 214.67 (x, y and z coordinates respectively) for α -amylase. For α -glucosidase, $x=59\text{\AA}$, $y=57\text{\AA}$ & $z=53\text{\AA}$, and centre 10.48, -7.04 and -19.76 (x, y and z coordinates respectively). After successful docking in Vina, the pose with lowest energy of binding or binding affinity was extracted and aligned with the receptor structure.

Statistical analysis

Data are presented as the mean \pm SD of triplicate determinations. Data were analysed by using a statistical software package (SPSS for Windows, version 22, IBM Corporation, NY, USA) using Tukey's-HSD multiple range *post-hoc* test. Values were considered significantly different at $p < 0.05$.

References

- Ibrahim MA, Islam MS. 2014. Butanol fraction of *Khaya senegalensis* root modulates β -cell function and ameliorates diabetes-related biochemical parameters in a type 2 diabetes rat model. J. Ethnopharmacol. 154, 832-838. <https://doi.org/10.1016/j.jep.2014.05.011>.
- Kim YM, Jeong YK, Wang MH, Lee WY, Rhee HI. 2005. Inhibitory effects of pine bark extract on alpha-glucosidase activity and postprandial hyperglycemia. Nutrition. 21: 756-761. <https://doi.org/10.1016/j.nut.2004.10.014>.

- McCue P, Shetty K. 2004. Inhibitory effects of rosmarinic acid extracts on porcine pancreatic amylase *in vitro*. Asian Pac. J. Clin. Nutr. 13: 101-106.
- Trott O, Olson AJ. 2010. AutoDock Vina: improving the speed and accuracy of docking with a new scoring function, efficient optimization and multithreading, J. Comput. Chem. 31: 455-461. [https://doi: 10.1002/jcc.21334](https://doi.org/10.1002/jcc.21334).